Conformational Studies by Circular Dichroism, ^{1}H NMR, and Computer Simulations of Bombolitins I and III in Aqueous Solution Containing Surfactant Micelles†

Eleni Bairaktari,‡ Dale F. Mierke,§ Stefano Mammi, and Evaristo Peggion*

Biopolymer Research Center, Department of Organic Chemistry, University of Padova, Via Marzolo 1, 35131 Padova, Italy

Received January 17, 1990; Revised Manuscript Received June 28, 1990

ABSTRACT: The heptadecapeptides bombolitin I and bombolitin III are two members of a series of biologically active peptides postulated to be membrane active. In order to understand the effects of the membrane on the secondary structure of the peptides, we have carried out the conformational characterization of bombolitins I and III in the presence of SDS micelles using circular dichroism, nuclear magnetic resonance, and computer simulations. The characteristic bands in the circular dichroism spectra indicate an α-helix content of approximately 60% in bombolitin III and 70% in bombolitin I. The observation of NOE's quite distinctive for such secondary structure strongly supports the CD results. The conformational preferences of the two bombolitins derived from CD and NMR were then energetically refined with molecular dynamics simulations. The results from the spectroscopic examination were utilized as input for the simulations, the CD results for generation of the initial structure, and the NOE's as constraints during the simulations. The results from the different techniques employed are in complete agreement.

Quite recently, five structurally related heptadecapeptides rich in hydrophobic residues have been isolated from the venom of a bumblebee. These materials have been fully characterized in terms of biological properties by Argiolas and Pisano (1985), who named them "bombolitins". All bombolitins are structurally and functionally very similar. They lyse erythrocytes

Bombolitin I	I-K-I-T-T-M-L-A-K-L-G-K-V-L-A-H-V-NH_2
Bombolitin II	S-K-I-T-D-I-L-A-K-L-G-K-V-L-A-H-V-NH_2
Bombolitin III	I-K-I-M-D-I-L-A-K-L-G-K-V-L-A-H-V-NH_2
Bombolitin IV	I-N-I-K-T-I-L-A-K-L-V-K-V-L-G-H-V-NH_2
Bombolitin V	I-N-V-L-G-I-L-G-L-L-G-K-A-L-S-H-L-NH_2

and liposomes and enhance the activity of the calcium-dependent enzyme phospholipase A_2. Interestingly, the same biological properties are exhibited by other natural occurring peptides, such as crabrolin (Argiolas & Pisano, 1984), melittin (Habermann, 1972), and mastoparan (isolated from bee's venom) (Hirai et al., 1979), which have a completely different primary structure. This unusual circumstance of peptides with different amino acid sequences performing the same biological action suggests that they share common conformational features.

Many of these peptides may adopt amphiphilic α-helical secondary structures. The amphiphilic nature could of course account for the accessibility of these peptides to membranes. The importance of the amphiphilic helix as a determinant of the biological properties of peptide hormones and toxins was stressed years ago by Kaiser and Kezdy (1983). It is therefore of importance to determine the conditions in which amphiphilic helices are formed and to study the interaction of amphiphilic peptides with membranes, with micelles, and eventually with phospholipase A_2. Along these lines, we have undertaken conformational examination of the series of bombolitins using circular dichroism, high-resolution nuclear magnetic resonance, and computer simulations. Here we report the results from the investigation of bombolitins I and III in the presence of sodium dodecyl sulfate (SDS)[1] used as a mimetic for biological membranes. The determination of the preferred secondary structure of these biologically important peptides, within an environment similar to that of a membrane, may lend insight into their biological action. In the accompanying paper (Bairaktari et al., 1990a), the conformational preferences of bombolitins I and III in aqueous solutions are reported.

Experimental Procedures

Bombolitins I and III were synthesized by the solid-phase Merrifield procedure and purified by HPLC. The final products exhibited single peaks in the HPLC profile with different eluting systems and correct amino acid ratios in enzymatic and acid hydrolysates.

Circular dichroism (CD) spectra were obtained on a Jasco Model J-600A automatic recording spectropolarimeter interfaced and controlled by a PC. The measurements were performed at room temperature in quartz cells of 0.1- and 0.001-cm path length. Spectra were obtained with a 1-nm bandwidth, scan speed of 10 nm/min, and time constant of 8 s. Two scans were obtained to improve the signal to noise ratio. The air base line was recorded and subtracted after each spectrum. All CD spectra are reported in terms of ellipticity units per mole of peptide residue ($[\theta]_R$).

The NMR experiments were performed at 313 K on a Bruker AM 400 spectrometer and the data processed on a Bruker X-32 workstation. Peak positions were measured

† A preliminary account of this work was presented at the 11th American Peptide Symposium, July 9–14, 1989, La Jolla, CA. This work was supported in part by the National Research Council (CNR) of Italy.

* To whom correspondence should be addressed.

‡ Present address: Laboratory of Analytical Biochemistry, University Hospital, Ioannina, Greece.

§ Present address: Organisch-Chemisches Institut, Technische Universität München, Garching, FRG.

[1] Abbreviations: NMR, nuclear magnetic resonance; CD, circular dichroism; SDS, sodium dodecyl sulfate; NOE, nuclear Overhauser enhancement; HOHAHA, homonuclear Hartmann–Hahn spectroscopy; NOESY, two-dimensional nuclear Overhauser enhancement spectroscopy; PC, personal computer; cmc, critical micellar concentration; HPLC, high-performance liquid chromatography.

0006-2960/90/0429-10090$02.50/0

relative to tetramethylsilane as internal standard. The NMR samples contained 2.5 mM bombolitin I or 2.56 mM bombolitin III in either H_2O (10% ^2H_2O) or ^2H_2O at pH 4.1 (uncorrected), in the presence of 0.32 M SDS-d_{25} (MSD Isotopes) and 10 mM phosphate buffer. CD spectra of the solutions used for the NMR studies were recorded both before and after the experiments. The spectra were identical with those obtained at lower concentrations.

Pure absorption two-dimensional homonuclear ^1H NMR spectra were obtained according to the TPPI method (Drobny et al., 1979; Bodenhausen et al., 1980) with 256–512 experiments of 2K data points. Prior to Fourier transformation the time domain data were multiplied by phase-shifted sine-bell or Gaussian window functions in both dimensions, and zero filling to 2K × 2K real points was carried out. Third-order polynomial base-plane correction was performed after transformation.

The 2D homonuclear Hartmann–Hahn (HOHAHA) spectra were obtained with the sequence described by Bax and Davis (1985). The MLEV-17 spin-locking sequence was cycled 44–48 times with trim pulses of 2.5 ms each, for total mixing times of 75–81 ms. Typically, spin-locking fields of 10 kHz were utilized. For measurements in H_2O, 1,1–ECHO observation pulses were employed (Bax et al., 1987; Sklenar & Bax, 1987). Delays of 178 and 334 μs were used for the 1,1 and ECHO, respectively. Two-dimensional NOESY spectra were recorded with the standard sequence with a mixing time of 200 ms (Bodenhausen et al., 1984). For suppression of the H_2O signal, selective irradiation during the relaxation delay and mixing time and a 1,1 observation pulse (delay 178 μs) were employed (Wider et al., 1983; Plateu & Gueron, 1982). Double quantum (DQ) correlated spectra were recorded in ^2H_2O with a preparation period of 15 ms (Maceri & Freeman, 1983; Boyd et al., 1985).

The molecular dynamics and energy minimizations were carried out with the XPLOR simulation package (Brünger, 1988). The potential energy is expressed as a sum of terms describing the deformation of bond lengths, angles, and torsions and nonbonded interactions, including a term for hydrogen bonds. Two modifications of the potential parameters were deemed necessary: (1) the force constant of the ω torsion was reduced from 300 to 20 kcal/mol and (2) the phase shift of the energy expression for the ϕ torsion was adjusted to obtain minima at 60°, 180°, and −60°, instead of 0°, 120°, and −120°. Both of these adjustments are in line with parameters commonly employed (Momany et al., 1975; Weiner et al., 1984; Hagler, 1985).

A square-well term was added to the energetic expression for the description of the measured NOE's. The distance constraints for the square-well NOE term were 1.8 Å for the lower bounds while the strengths of the NOE, determined from the volume of the cross peak in the NOESY spectra, were the criteria for the upper bounds (strong, 2.7 Å; medium, 3.3 Å; weak, 5.0 Å). The NOE term was only effective when the distance between the two protons was outside of this range, e.g., for a strong NOE, 1.8–2.7 Å. For methylene and methyl groups, all of the protons were used in the NOE constraints with the upper bounds increased by 0.5 Å. Lists of the restraints are given in Tables I and II. The force constants for the NOE term were varied during the simulations as described below. Energy minimizations were carried out with the Powell method until derivatives were less than 0.01 kcal/(mol·Å^2) (Powell, 1979). The simulations were carried out on a VAX 8650 with each picosecond (1000 steps) of dynamics taking approximately 0.3 h of cpu.

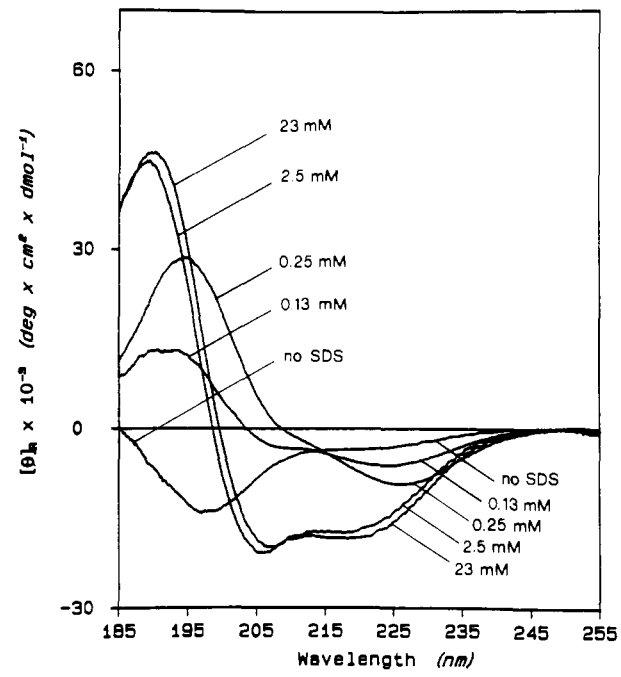

FIGURE 1: Circular dichroism spectra of bombolitin III in aqueous solution (3.89×10^{-5} M, pH 5.0) with increasing concentration of SDS (indicated).

The molecular dynamic simulations were run for 20 ps at a temperature of 300 K. An α-helix (ϕ, ψ = −65°, −45°, with all other torsions 180°) was chosen as the starting structure. Velocities were applied to the system in a Maxwellian distribution to obtain the desired temperature. A period of 2 ps with a step size of 0.5 fs preceding the simulation was used to introduce the NOE's and allow the system to equilibrate to the temperature. The force constants for the NOE's were slowly incremented during the equilibration. The strong NOE's were applied first with a force constant of 0.8 kcal/(mol·Å^2). After 200 steps (0.1 ps), the force constants were doubled, and this process was repeated 10 times (total 1 ps) with a maximum force constant of 100 kcal/(mol·Å^2). During the second picosecond of equilibration this process was repeated for the medium and weak NOE's, while the 100 kcal/(mol·Å^2) force constant was maintained on the strong NOE's. After the equilibration period all of the NOE force constants were then set to 20 kcal/(mol·Å^2), and the simulation was continued for 20 ps with a step size of 1.0 fs. To examine the energetics of the obtained structure, the NOE constraints were removed and the dynamics continued for an additional 10 ps.

Results and Discussion

CD Measurements. The CD spectra from a titration of an aqueous solution of bombolitin III (3.89×10^{-5} M, pH 5.0) with SDS are shown in Figure 1. The CD spectrum of the dilute solution without SDS indicates that the peptide lacks well-defined secondary structure but is not completely random. This is revealed by the broad negative shoulder at 222 nm and low intensity of the negative band below 200 nm.

With the addition of SDS, at concentrations below the critical micellar concentration (cmc), the spectra show an increase in secondary structure. The on-set of secondary structure is evident with a ratio of peptide to SDS of 1:3.3 and 1:6.4 (Figure 1, [SDS] = 0.13 mM and 0.25 mM, respectively). The shape of the CD pattern and, specifically, the minimum at 228 nm indicate that there is a component of type II β-turn in the secondary structure (Deslaurier et al., 1981). At SDS concentrations above the cmc, the peptide tends to

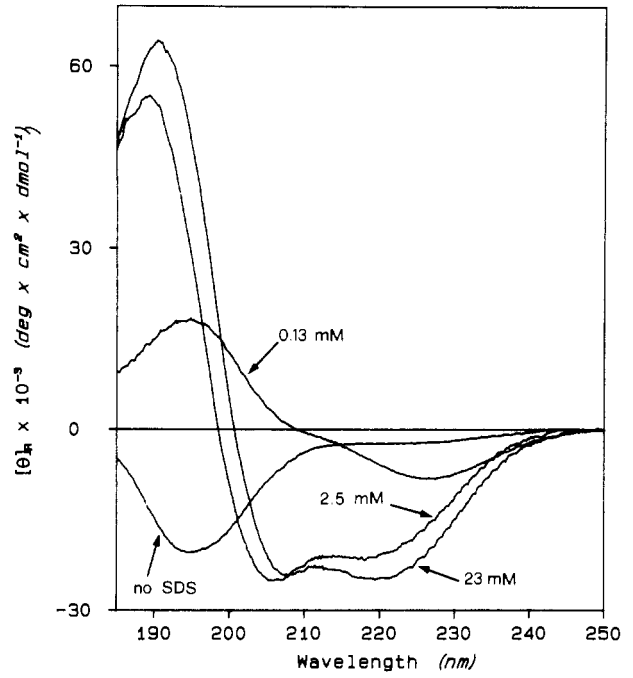

FIGURE 2: Circular dichroism spectra of bombolitin I in aqueous solution (2.92×10^{-5} M, 10 mM phosphate buffer, pH 5.0) with increasing concentration of SDS (indicated).

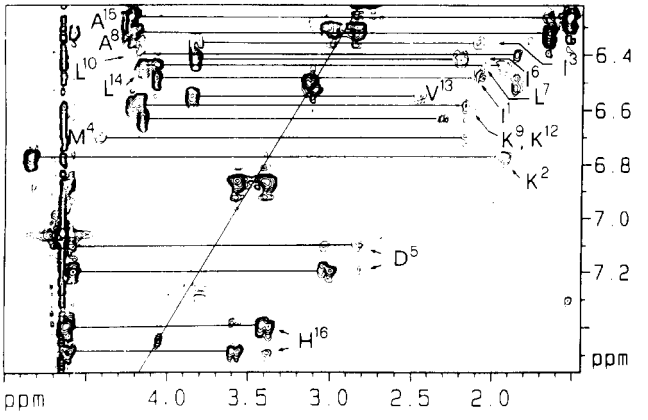

FIGURE 3: Expanded portion of a ^{1}H 2D double quantum experiment at 400 MHz of bombolitin III (2.56 mM with 320 mM perdeuteriated SDS) in ^2H_2O. The $C^\alpha H$–$C^\beta H$ connectivities are illustrated.

fold into an α-helical conformation. At a ratio of about 1:1 peptide to micelles, the peptide is approximately 60% α-helical. Upon further addition of SDS this conformation is maintained. This indicates that all the peptide is associated with the SDS. In the micelle-bound state, the peptide conformation is completely pH independent up to pH 8.5. This finding is in agreement with the conclusion that the peptide is completely associated with the SDS micelles.

Very similar results were obtained with bombolitin I (Figure 2). In this case the helix content of the peptide in the micelle-bound state, estimated from the amplitude of the negative CD band at 222 nm, is of the order of 70%, i.e., a little higher than in the case of bombolitin III.

NMR Measurements. The proton resonances of bombolitins I and III were assigned by use of phase-sensitive COSY, DQ correlated spectroscopy, and HOHAHA experiments. The results of some typical experiments on bombolitin III are shown in Figures 3–7. The two-dimensional double quantum spectrum in ^2H_2O allowed the identification of all of the $C^\alpha H$–$C^\beta H$ correlations (Figure 3), some of which were not well resolved in the COSY spectrum. To identify the complete spin systems of the amino acids, two-dimensional HOHAHA spectra were

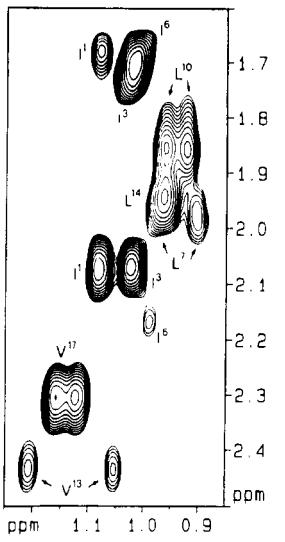

FIGURE 4: Aliphatic region of a HOHAHA spectrum at 400 MHz of bombolitin III (2.56 mM with 320 mM perdeuteriated SDS) in ^2H_2O. The resonances from the methyl groups of Val, Ile, and Leu are identified.

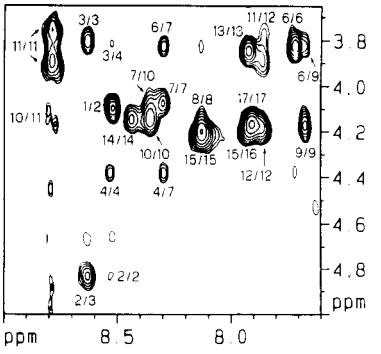

FIGURE 5: Fingerprint region of a pure-phase NOESY spectrum at 400 MHz of bombolitin III (2.56 mM with 320 mM perdeuteriated SDS) in H_2O (10% ^2H_2O). A mixing time of 200 ms was employed.

collected with relatively long mixing times. The high-field region of a HOHAHA spectrum in ^2H_2O is shown in Figure 4, illustrating the spin systems of several side chains. These experiments allowed the identification of the aliphatic regions of the amino acid spin systems.

The correlation of the NH protons with the aliphatic resonances and the sequential assignment of the residues were carried out with HOHAHA and NOESY spectra in H_2O. In the HOHAHA spectrum, each of the residues displays a cross peak between the NH and the $C^\alpha H$ with the exception of Ile^1, due to fast exchange with the solvent, and Asp^5, which is bleached out from the suppression of the solvent peak (data not shown). The observation of short distances between $C^\alpha H(i)$ and $NH(i)$ and between $C^\alpha H(i)$ and $NH(i+1)$ from the NOESY spectra (see Figure 5) was utilized for the sequential assignments of the amino acids. These assignments were further confirmed by the $NH(i)$–$NH(i+1)$ (shown in Figure 6) and $C^\beta H(i)$–$NH(i+1)$ NOE's.

A single set of resonance lines was observed for each spin system. Taking into account that under our experimental conditions the peptide is completely bound to micelles, this indicates that a single conformation is assumed by bombolitin III upon association with the SDS micelles.

The observed NOE's are shown in Table I. These findings are in agreement with the CD results. The presence of strong $NH(i)$–$NH(i+1)$ NOE's over the full length of the molecule of bombolitin III is indicative of a helical structure (Wüthrich et al., 1984). Even stronger evidence of such secondary

Table I: Observed Nuclear Overhauser Effects for Bombolitin III in the Presence of Sodium Dodecyl Sulfate Micelles[a]

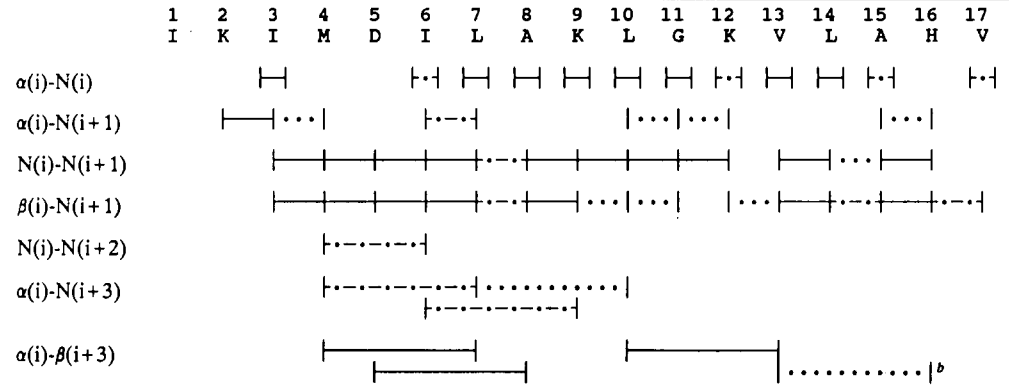

[a] Strength of NOE calculated from volume of the cross peak observed in NOESY spectra: (—) strong; (-·-) medium; (···) weak. [b] This NOE was very weak and was not utilized as a restraint during the molecular dynamics.

Table II: Observed Nuclear Overhauser Effects for Bombolitin I in the Presence of Sodium Dodecyl Sulfate Micelles[a]

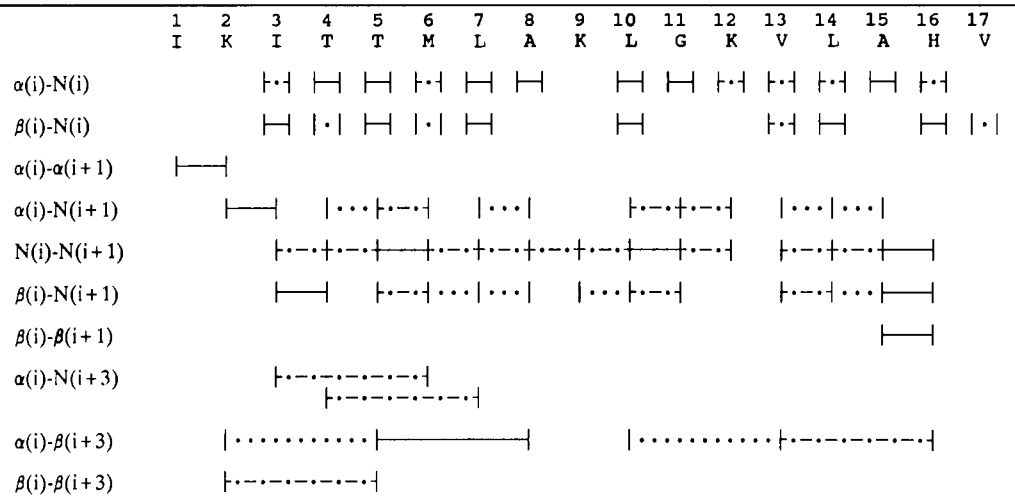

[a] Strength of NOE calculated from volume of the cross peak observed in NOESY spectra: (—) strong; (-·-) medium; (···) weak.

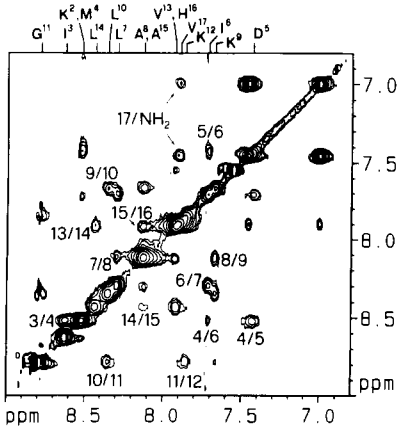

FIGURE 6: NH–NH region of a pure-phase NOESY spectrum at 400 MHz of bombolitin III (2.56 mM with 320 mM perdeuteriated SDS) in H_2O (10% ^2H_2O).

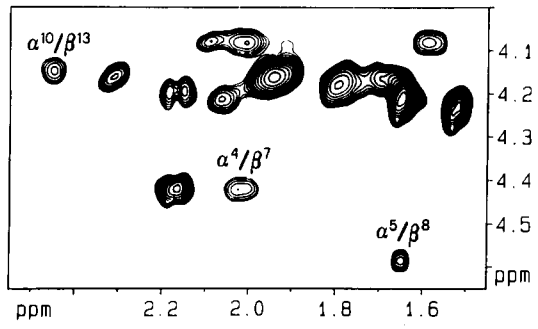

FIGURE 7: Aliphatic region of a pure-phase NOESY spectrum at 400 MHz of bombolitin III (2.56 mM with 320 mM perdeuteriated SDS) in ^2H_2O. The $C^{\alpha}H(i)$–$C^{\beta}H(i+3)$ NOE's are illustrated.

structure is the short distances of the type (i)–$(i+2)$ and (i)–$(i+3)$ observed. Specifically, strong connectivities between $C^{\alpha}H(i)$ and $C^{\beta}H(i+3)$ extend from Met[4] to Val[13] (Figure 7). In addition, a very weak cross peak is observed between Val[13] $C^{\alpha}H$ and His[16] $C^{\beta}H_2$ (not shown). Moreover, a connectivity is found between NH(4) and NH(6) (Figure 6). These results indicate that the helical segment starts with Met[4] and extends at least to Val.[13]

Similar NMR studies were carried out on bombolitin I in the micelle-bound state. Also in this case, the spin system of all individual amino acids has been identified with two-dimensional NMR experiments. The most significant results of NOESY experiments relevant for the identification of the secondary structure are reported in Figures 8–10. Connectivities of the type $NH(i)$–$NH(i+1)$ were observed for the majority of the peptide sequence (Figure 9). In addition, four $C^{\alpha}H(i)$–$C^{\beta}H(i+3)$ (Figure 10) and two $C^{\alpha}H(i)$–$NH(i+3)$ (Figure 8) were observed. The NOE's that could be unambiguously assigned are listed in Table II. These results suggest that the helical segment starts with Ile[3] and extends at least to Ala[15]. Therefore, also in this case the helical segment comprises the central sequence of the peptide chain, and consistent with CD data, its length is slightly higher than in

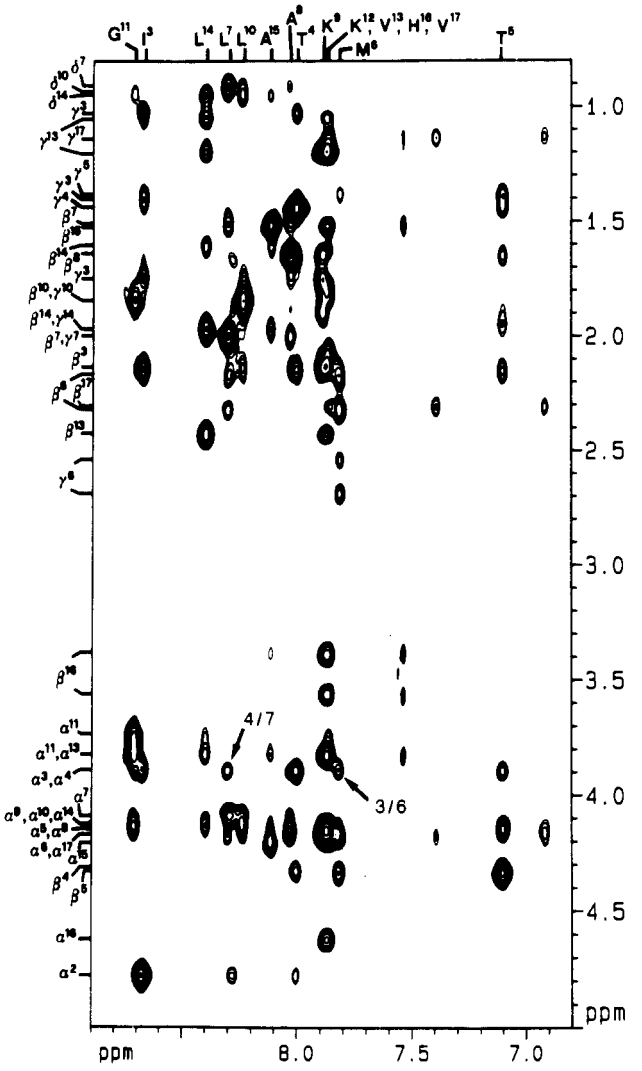

FIGURE 8: NH–aliphatic region of a NOESY spectrum at 400 MHz of bombolitin I (2.5 mM with 320 mM perdeuteriated SDS, pH 4.1) in H_2O (10% ^2H_2O).

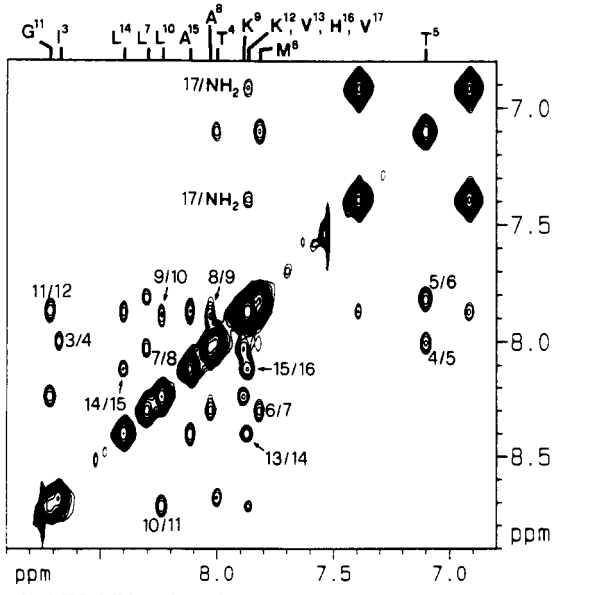

FIGURE 9: NH–NH region of a pure-phase NOESY spectrum at 400 MHz of bombolitin I (2.5 mM with 320 mM perdeuteriated SDS, pH 4.1) in H_2O (10% ^2H_2O).

bombolitin III. Again, it is important to note that only one set of resonances were observed, indicative of a single conformation of bombolitin I in the micelle-bound state.

Table III: Selected Dihedral Torsions (deg) of Bombolitins III and I from Molecular Dynamics Simulations

		bombolitin III structures from molecular dynamics		bombolitin I structures from molecular dynamics	
residue	torsion	after 20 ps	extended for 10 ps	after 20 ps	extended for 10 ps
Ile[1]	ψ	−61	−61	161	154
	χ_1	−63	−62	−72	−85
Lys[2]	ϕ	−48	−46	−105	−97
	ψ	−44	−64	24	−67
	χ_1	−172	−177	−155	178
Ile[3]	ϕ	−60	−53	−50	−49
	ψ	−36	−53	−35	−18
	χ_1	−69	−72	−69	−65
Met[4] (Thr[4])	ϕ	−79	−54	−52	−54
	ψ	−42	−54	−44	−37
	χ_1	−56	−50	179	171
Asp[5] (Thr[5])	ϕ	−56	−56	−57	−60
	ψ	−49	−69	−38	−46
	χ_1	145	176	162	179
Ile[6] (Met[6])	ϕ	−68	−56	−65	−56
	ψ	−53	−45	−49	−35
	χ_1	−71	−49	−74	−59
Leu[7]	ϕ	−51	−68	−64	−49
	ψ	−36	−50	−53	−56
	χ_1	−164	−168	−59	−61
Ala[8]	ϕ	−72	−50	−47	−45
	ψ	−56	−49	−62	−61
	χ_1	−49	−65	−67	−48
Lys[9]	ϕ	−59	−71	−62	−56
	ψ	−51	−54	−51	−58
	χ_1	−66	−79	−171	−17
Leu[10]	ϕ	−67	−53	−58	−53
	ψ	−56	−55	−45	−53
	χ_1	−167	−164	−67	−50
Gly[11]	ϕ	−52	−54	−68	−47
	ψ	−47	−65	−65	−61
Lys[12]	ϕ	−63	−49	−48	−64
	ψ	−50	−65	−56	−55
	χ_1	176	−178	178	−16
Val[13]	ϕ	−54	−49	−59	−59
	ψ	−48	−53	−54	−42
	χ_1	−167	−179	178	172
Leu[14]	ϕ	−58	−61	−59	−63
	ψ	−45	−40	−40	−46
	χ_1	162	−167	−71	−79
Ala[15]	ϕ	−60	−59	−76	−13
	ψ	−43	−57	−72	63
	χ_1	−64	−59	−66	177
His[16]	ϕ	−179	−162	−63	168
	ψ	172	177	−64	−45
	χ_1	61	66	177	162
Val[17]	ϕ	−53	−53	110	65
	χ_1	164	172	−74	−61

An important and unexpected difference with respect to bombolitin III is the presence of a clear and strong NOE cross peak between the $C^{\alpha}H$ protons of Ile[1] and Lys[2] (Figure 10). This peak is diagnostic for the presence of a cis peptide configuration (Arseniev et al., 1983). To our knowledge, this is the first time that a cis amide bond not involving a proline residue is found in a linear peptide (Bairaktari et al., 1990b). Cis amide isomers have been observed within cyclic peptides (Mierke et al., 1989). No trace of the trans isomer was detected.

Our findings do not allow the characterization of the interaction of bombolitins I and III with the micelle. However, due to the amphiphilic character of the helices, it is very likely that the helix axis is oriented parallel to the surface of the micelle, with the hydrophobic side chains directed inward, interacting with the hydrocarbon moiety of the surfactant

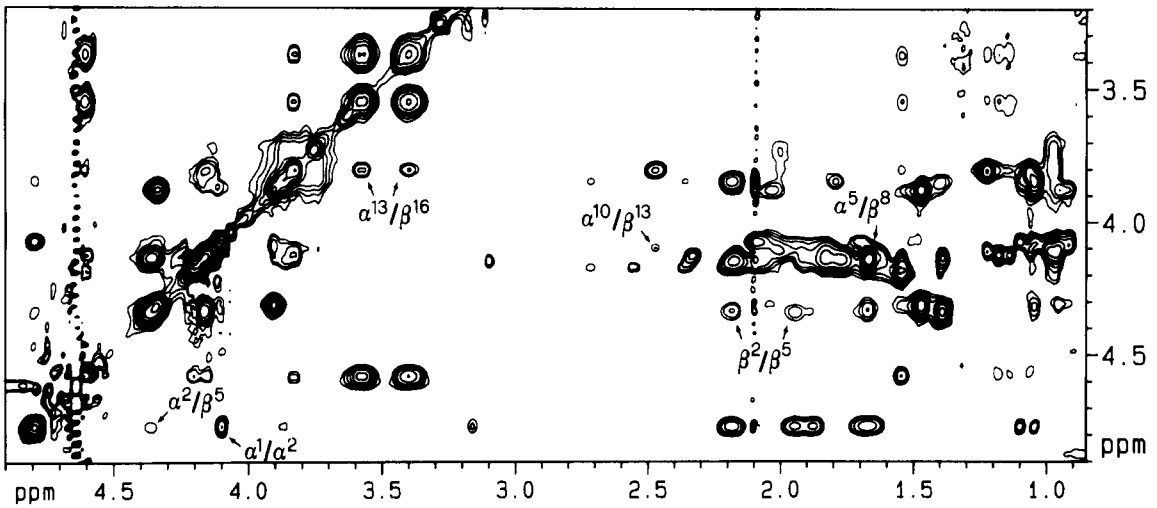

FIGURE 10: Aliphatic region of a pure-phase NOESY spectrum at 400 MHz of bombolitin I (2.5 mM with 320 mM perdeuteriated SDS, pH 4.1) in ^2H_2O. The $C^{\alpha}H(i)$–$C^{\beta}H(i+3)$ NOE's and the $C^{\alpha}H(1)$–$C^{\alpha}H(2)$ peak are illustrated.

molecules. This type of arrangement would provide an explanation for the cis amide linkage between Ile[1] and Lys[2] in bombolitin I. Certainly, the association of the peptide with the micelle must account for the presence of the cis bond, since this isomer is not found in the absence of detergent (see accompanying paper).

The requirement to be met is that the α-amino group of Ile[1] and the ϵ-amino group of Lys[2] must be on the surface of the micelle to maintain the strong electrostatic interaction with the negatively charged sulfate groups of SDS. In addition, the side chains of Ile[1] and Lys[2] must be placed in opposite directions. Model studies indicate that a cis peptide configuration would facilitate such a disposition. This spatial arrangement is also possible with a trans peptide configuration, by a proper selection of ψ_1 and ϕ_2 dihedral angles. However, these values would be outside the low-energy regions of (ϕ, ψ) conformational space usually associated with amino acids (Zimmermann et al., 1977). The favorable displacement of the side chains overcomes the energy difference usually associated with cis and trans amide isomers (i.e., trans isomers 2–3 kcal more favorable).

It is worth noting that the same cis peptide configuration is not observed in bombolitin III under analogous conditions. The only significant difference in the sequence of the two peptides appears to be the presence in bombolitin III of Asp instead of Thr at position 5. It is possible that the side-chain carboxylate group of the Asp[5] residue forms a salt bridge with the ϵ-amino group of Lys[2] or with the α-amino group of Ile[1]. In such a case, the ion pair is not forced to stay on the surface of the micelle, and a cis peptide configuration is not needed.

This explanation is a working hypothesis, and further work is needed to clarify the problem. We are currently examining NMR experiments that may allow for a more thorough understanding of this intermolecular interaction and the driving forces present.

Computer Simulations. To energetically refine the experimentally determined structure, 20 ps of NOE-restrained molecular dynamics was carried out on both bombolitins. Since the data from the experimental conformational analysis of both sequences in the presence of SDS clearly indicate a large extent of α-helix, such a structure was chosen as the starting point for the energetic refinement. The utilization of the experimental data to define a starting structure greatly facilitates the simulations. It is not necessary to carry out a costly search for the global minimum, which may not be the conformation adopted under the conditions under consideration, e.g., membrane-like environment. The goal of the simulations is to refine the experimentally determined structure with the energetic description of the molecular mechanics program. Indeed, many of the NOE's were satisfied with the starting α-helical structure.

In the case of bombolitin III the RMS difference of the NOE's (between the target distance and actual distance between the protons) was 0.20 Å. The slow application of the NOE's during the equilibration period allowed for the adjustment of the conformation to meet all of the NOE constraints, except for one (Lys[2] $C^{\alpha}H \rightarrow$ Thr[3] NH; target distance 2.4 ± 0.3 Å, actual distance 3.2 Å). The resulting RMS difference for the 57 constraints was 0.11 Å. The difference between the starting structure and the conformation after the equilibration period is relatively small, with an RMS difference between all of the atoms of 0.35 Å (main-chain atoms 0.23 Å).

In Table III the torsional angles ϕ, ψ, and χ_1 of the structure after the 20 ps of molecular dynamics are shown. This structure has an RMS difference of the NOE constraints and target values of 0.13 Å. The central portion of the α-helix is maintained during the dynamics and extends from residue 4 to residue 15. There is a little distortion, or unwinding of the helix, at both ends. This is in complete accord with the experimentally determined structure, namely, the observation of the NOE's.

As an approach to investigate the effects of the constraints during the simulations, an additional 10 ps of dynamics was carried out without the application of the NOE's. The torsions of the structure obtained from this extension of the dynamics are given in Table III. There are only minor differences between the structures after 20 ps and this extension. The RMS differences of all the atoms is 0.76 Å (main-chain atoms 0.69 Å). The relatively small difference found with and without the NOE's indicates that the derived structure is indeed very much the same and that the application (and fulfillment) of the NOE restraints did not cause great distortions in the structure.

The same procedure was followed for bombolitin I. After 20 ps of simulation, the NOE constraints are well satisfied, with an RMS difference of the actual distance and target values of 0.088 Å. During the equilibration period, with the application of the NOE constraints, the ω torsion angle between Ile[1] and Lys[2] adopts a cis arrangement, satisfying the strong NOE's between these two residues. The difference between the starting and final (after 20 ps) structures is rather

minor: the RMS difference is 1.7 Å (1.8 Å for main-chain atoms). This difference can be chiefly attributed to the unwinding of the helix at both ends (in addition to the formation of the cis ω torsion at the N-terminus): the RMS difference is 0.39 Å for residues 3–14 and 0.36 Å for the main-chain atoms. In Table III, the ϕ, ψ, and χ_1 values of the resulting structure are given. The backbone torsions of residues 3–14 are close to the standard values for the α-helix (the Ala^{15} and His^{16} torsions are slightly distorted from these values).

The molecular dynamics were then extended for an additional 10 ps without the application of the NOE's. The torsions of the resulting structure are also given in Table III. Again, there are minor differences between the structures after 20 ps and this extension: the RMS difference of all the atoms is 1.02 Å (1.1 Å for the main-chain atoms). The largest differences can be seen in the torsions of the end residues (note Ile^3, Ala^{15}, and His^{16}), indicating the unraveling of the α-helix without the NOE constraints.

Registry No. SDS, 151-21-3; bombolitin I, 95648-97-8; bombolitin III, 95732-42-6.

References

Argiolas, A., & Pisano, J. J. (1984) *J. Biol. Chem. 259*, 10106–10111.

Argiolas, A., & Pisano, J. J. (1985) *J. Biol. Chem. 260*, 1437–1444.

Arseniev, A. S., Kondakov, V. I., Maiorov, V. N., Volkova, T. M., Grishin, E. V., Bystrov, V. F., & Ovchinnikov, Yu. A. (1983) *Bioorg. Khim. 9*, 768–793.

Bairaktari, E., Mierke, D. F., Mammi, S., & Peggion, E. (1990a) *Biochemistry* (following paper in this issue).

Bairaktari, E., Mierke, D. F., Mammi, S., & Peggion, E. (1990b) *J. Am. Chem. Soc. 112*, 5383.

Bax, A., & Davis, D. (1985) *J. Magn. Reson. 65*, 355–360.

Bax, A., Sklenar, V., Clore, G. M., & Gronenborn, A. M. (1987) *J. Am. Chem. Soc. 109*, 6511–6513.

Bodenhausen, G., Vold, R. L., & Vold, R. R. (1980) *J. Magn. Reson. 37*, 93–106.

Bodenhausen, G., Kogler, H., & Ernst, R. R. (1984) *J. Magn. Reson. 58*, 370–388.

Boyd, J., Dobson, C. M., & Redfield, C. (1985) *J. Magn. Reson. 62*, 543–550.

Brünger, A. T. (1988) *XPLOR SOFTWARE*, President & Fellows Harvard University, Cambridge, MA.

Deslaurier, R., Evans, D. J., Leach, S. J., Meinwald, Y. C., Minasian, E., Nemethy, G., Rae, I. D., Scheraga, H. A., Somorjai, R. L., Stimson, E. R., Van Nispen, J. W., & Woody, R. W. (1981) *Macromolecules 14*, 985–996.

Drobny, G., Pines, A., Sinton, S., Weitekamp, D., & Wemmer, D. (1979) *Symp. Faraday Soc. 13*, 49–55.

Habermann, E. (1972) *Science 117*, 314–322.

Hagler, A. T. (1985) in *The Peptides* (Hruby, V., Udenfriend, S., & Meienhofer, J., Eds.) Vol. 7, pp 241–296, Academic Press, Orlando, FL.

Hirai, Y., Yasuhara, T., Yoshida, H., Nakajima, T., Fujino, M., & Kitada, C. (1979) *Chem. Pharm. Bull. 27*, 1942–1944.

Kaiser, E. T., & Kezdy, F. J. (1983) *Proc. Natl. Acad. Sci. U.S.A. 80*, 1137–1143.

Maceri, T. H., & Freeman, R. (1983) *J. Magn. Reson. 51*, 531–535.

Mierke, D. F., Yamazaki, T., Said-Nejad, O. E., Felder, E. R., & Goodman, M. (1989) *J. Am. Chem. Soc. 111*, 6847–6849.

Momany, F. A., McGuire, R. F., Burgess, A. W., & Scheraga, H. A. (1975) *J. Phys. Chem. 79*, 2361–2381.

Plateau, P., & Gueron, M. (1982) *J. Am. Chem. Soc. 104*, 7311–7312.

Powell, M. J. D. (1979) *Math. Programming 12*, 241–254.

Sklenar, V., & Bax, A. (1987) *J. Magn. Reson. 74*, 469–479.

Weiner, S. J., Kollman, P. A., Case, D. A., Chandra Singh, U., Ghio, C., Alagona, G., Profeta, S., & Weiner, P. (1984) *J. Am. Chem. Soc. 106*, 765–784.

Wider, G., Hasur, F. V., & Wüthrich, K. (1983) *J. Magn. Reson. 58*, 370–388.

Wüthrich, K., Billeter, M., & Braun, W. (1984) *J. Mol. Biol. 180*, 715–740.

Zimmermann, S. S., Pottle, M. S., Nemethy, G., & Scheraga, H. A. (1977) *Macromolecules 10*, 1–9.